Available online at www.sciencedirect.com
SCIENCE DIRECT®

Journal of Volcanology and Geothermal Research 156 (2006) 35 – 54

Journal of volcanology and geothermal research

www.elsevier.com/locate/jvolgeores

A morphometric analysis of the submarine volcanic ridge south-east of Pico Island, Azores

R.C. Stretch [a,*], N.C. Mitchell [b], R.A. Portaro [c]

[a] *Department of Geography, University of Cambridge, Downing Site CB2 3EN, UK*
[b] *Department of Earth Sciences, Cardiff University, PO Box 914, Cardiff CF10 3YE, UK*
[c] *Istituto di Scienze Marina, CNR, Via P. Gobetti 101, 40129 Bologna, Italy*

Received 20 May 2003; accepted 2 March 2006
Available online 23 May 2006

Abstract

A region of crustal extension, the Azores Plateau contains excellent examples of submarine volcanic edifices constructed over a wide range of ocean depths along the Pico Ridge. Using bathymetric data and Towed Ocean Bottom Instrument (TOBI) side-scan sonar imagery, we measured the dimensions (diameter, height, slopes), shape, and texture of these volcanic edifices to further understanding of the geometric development of a submarine ridge. Our analysis and interpretation of the measurement and texture data suggest the following: (1) the various edifice types do not correlate with depth ranges, suggesting that ambient water pressure is not a controlling factor in configuration of the edifice formed; (2) the cones have a mean diameter of 948 m, height of 152 m, and slope of 15.6°, and are peaked rather than displaying flat-topped summits; and (3) while hummocky-textured cones also occur, smooth-textured cones predominate. The cones seem to develop preferentially outwards, then upwards, with only a weak correlation between diameter and height, suggesting that the cone population does not evolve self-similarly. Although smooth and hummocky cone populations are not statistically different in mean slope angle and eruption depth, the hummocky cones have a significantly greater mean diameter than the smooth cones. We suggest that hummocky-textured cones (probably involving eruption of pillow lavas) are formed after voluminous smooth textured flows. Nearest-neighbour analysis suggests that submarine cones are distributed randomly whereas subaerial cones are not. We interpret this finding to suggest subaerial cones being masked by over-covering flows, which tend to flow further than submarine lava flows. Furthermore, the spatial distribution of cones away from the ridge centre is not easily explained by a magma supply fed via lava tubes from central eruptions, because of a lack of consistent pathway down gradient. Fissure vents seem to be important in determining construction of the ridge and result in linear arrangements of edifices and cone elongation, consistent with the regional tectonic trend of this part of the Azores Plateau. Cones form as each feeding dyke intrusion cools and the eruption becomes localized along point-source vents along the fissure. The ridge seems to be predominantly formed from fissure eruptions along the ridge axis, with subordinate transport of lava down its flanks.

Keywords: submarine volcanism; bathymetry; morphometry; cones

1. Introduction

The Azores Plateau is unique in having many active volcanic ridges that encompass a remarkable range in scale and a wide range of water depths (Mitchell et al.,

* Corresponding author.
E-mail address: rcs29@cam.ac.uk (R.C. Stretch).

0377-0273/$ - see front matter
doi:10.1016/j.jvolgeores.2006.03.009

2003a,b); the Pico Ridge is no exception. Submarine volcanic ridges at spreading centres are important features because the magmatic flux associated with them is substantial (Zhang and Tanimoto, 1992): an estimated 62% by volume of the Earth's magmatic flux occurs along ocean ridges (Perfit and Davidson, 2000). Volcanic rift zones are also important structural components of ocean island volcanoes (Leslie et al., 2004), and studying the features associated with them may increase understanding of melting processes and transport of melt through the lithosphere to form oceanic crust (Mitchell et al., 2003a,b). The environment in which submarine volcanic eruptions occur is unique because of the thick oceanic crust and the overlying pressure of water (an increase of 1 MPa for every 100 m depth of water; Grosfils et al., 2000). However, features associated with submarine volcanic ridges are still poorly understood because of their relative inaccessibility. New imagery from high spatial resolution instruments combined with bathymetric data, offer increased potential for understanding volcanic ridges and how they relate to dyke emplacement, faulting and the style of eruption – whether gentle and effusive, or explosive (Head and Wilson, 2003). Studies of the features associated with the submarine ridges, including their number, size, shape, depth and texture can provide information on the geological processes that control crustal melt supply, the construction and evolution of oceanic crust and how tectonic and volcanic processes combine to sustain sea floor spreading (Edwards et al., 1991; Smith et al., 1995a,b; Smith and Cann, 1999; Parson et al., 2000; Smith et al., 2001).

Previous studies of volcanic features at ridges have been performed using similar techniques to those employed in this study, at the Mid-Atlantic Ridge (Critchley et al., 1994; German et al., 1996; Searle et al., 1997; Smith et al., 1997; Mitchell and Livermore, 1998; Searle et al., 1998; Parson et al., 1999; Briais et al., 2000; Gracia et al., 2000; Parson et al., 2000), East Pacific Rise (Fornari and Ryan, 1984; Sempere and Macdonald, 1986; Bicknell et al., 1987; MacDonald et al., 1988; Cowie et al., 1994), South-West Indian Ocean Ridge (Mendel and Sauter, 1997; Sauter et al., 2002), Reykjanes Ridge (Parson et al., 1993; Magde and Smith, 1995; Smith et al., 1995b), and Puna Ridge, Hawai'i (Smith and Cann, 1999). These studies have shown both similarities and differences in submarine morphology at the various slow-spreading ridge locations and differences in the nature of the associated volcanic processes have been inferred as a result.

In this paper, volcanic edifices on Pico Ridge have been mapped and classified using sonar imagery and have been measured and statistically analysed, to determine which factors regulate activity at the ridge. The aim of our investigation is to understand the volcanic and tectonic processes involved in the evolution of the ridge, and how the ridge develops geometrically at a variety of scales. The development of cones, in particular, is fundamental to crustal construction (Smith and Cann, 1990; Smith et al., 2001), hence the morphometry of cones is examined, to assess whether or not they develop self-similarly and if there is any relationship between their dimensions. The textures of features are also studied to constrain the nature of the magmatic processes occurring in the area and to infer local effusion rates. For example, a hummocky texture is believed to be associated with a slower, more effusive eruption (Gregg and Fink, 1995). The distribution of volcanic features on the ridges of the Azores Plateau is examined to assess the influence of tectonism on the ridge's development, as overall morphology is a result of volcanic construction and tectonic dismemberment (Blondel and Murton, 1997).

2. Study area

Volcanic ridges develop in regions of crustal extension, many of which are affected by crustal plumes or other regional melting anomalies. Geochemical and geophysical evidence (Zhang and Tanimoto, 1992; Moreira and Allegre, 2002), including low shear wave-velocity anomalies and Mantle Bouger Anomalies of 40–60 mGal (Luis et al., 1998; Thibaud et al., 1998) suggests that a mantle anomaly is active underneath the Azores triple junction where the American, Eurasian and African plates meet. In this region, the Mid-Atlantic Ridge displays an attenuated roughness, the ridge is shallower (Litvin, 1984; Miranda et al., 1991; Lourenco et al., 1998; Luis et al., 1998; Escartin et al., 2001) and the crust is 60% thicker than normal (Searle, 1980). The current model (Luis et al., 1998; Nunes, 2002) suggests that the Azores Plateau acts as an ultra slow spreading centre and a transfer zone between the Mid-Atlantic Ridge and the E–W Gloria fault, as it accommodates dextral shear movement between the Eurasian and African plates. African–Eurasian plate motion is oblique to the general trend of the Terceira rift. The deformation of the Azores Plateau is therefore a result of the combined effects of East–West spreading in the Mid-Atlantic Rift and strike slip motion on the Gloria

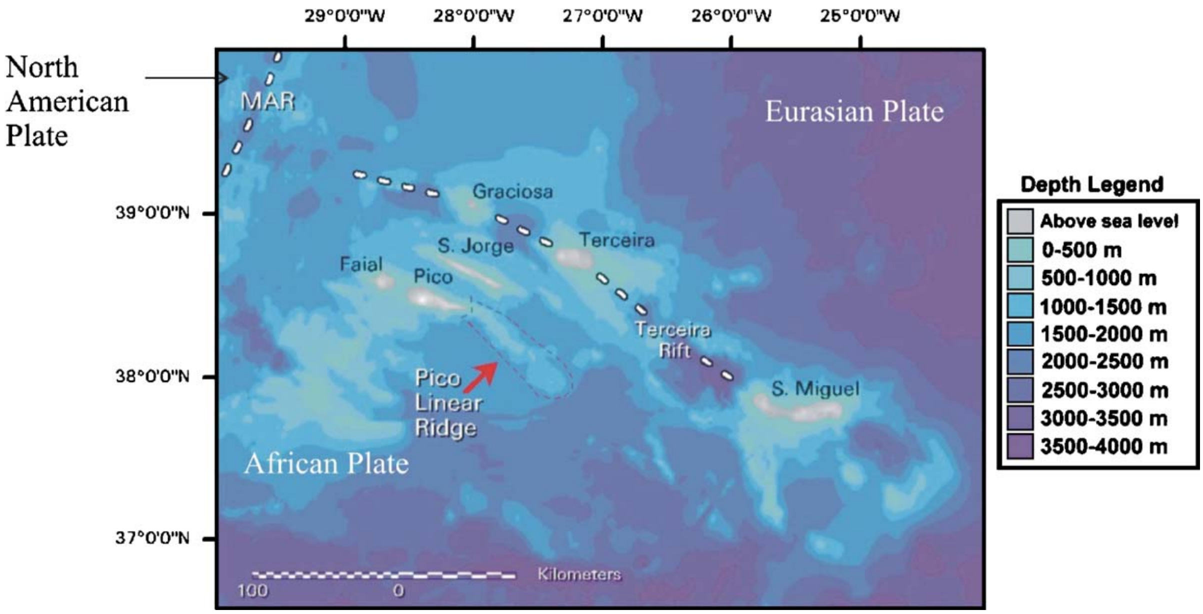

Fig. 1. Bathymetry of the Azores Plateau and location of Pico Ridge. The Mid-Atlantic ridge is visible to the northwest and the Terceira rift marks the boundary between the Eurasian and African plates. Adapted from Whitesides (2000).

Fault. Hence, deformation across the Azores is transtensional. Current deformation is concentrated in a band centred around the Terceira Axis, a zone of intense volcanism absorbing the movement between the Eurasian and African plates (Fig. 1) (Miranda et al., 1998).

Previous interpretations of the Azores triple junction (documented in Miranda et al. (1998) and Luis et al. (1998)) include the evolution of a ridge–fault–fault to a ridge–ridge–ridge system; migration of the triple junction due to a change in spreading direction and a leaky transform model. Initiation of the Azores spreading centre probably occurred at 36 Ma and in the past 7 Ma, spreading of the MAR was 22–25 mm/yr on an azimuth of 98°–108° (Ondreas et al., 1997; Cannat et al., 1999); the spreading rate at the Terceira rift is currently 3 mm/yr (Searle, 1980). There are currently two mechanisms that are believed to be deforming the Azores block (Miranda et al., 1998): the first mechanism is driven by successive jumps of the triple point and has generated activity along N120°E fractures and transform faults in the last 1 Ma; the other mechanism is associated with the N150°E trend in faulting and is active when the Azores Plateau is deformed by shear between the two plates.

The submarine ridges of the Azores Plateau are still not fully understood and are little studied – prior to the cruise which provided the data set for this study, only two studies had been performed in the area using instruments with much lower spatial resolution (Searle, 1980; Luis et al., 1998). Initial studies of the data suggested that the ridges are very similar to the axial volcanic ridges of the MAR, made up of many small cones (Ligi et al., 1999).

3. Data and methods

3.1. Data sets

Our research is based on side-scan sonar images of the morphology of the seafloor of the Azores plateau and bathymetric data sets. The data were collected on the AZ99 cruise from 30 June to 4 August 1999 onboard the R/V Urania, by using a 30 kHz sonar on TOBI (Towed Ocean Bottom Instrument) towed 400 m above the sea floor. TOBI images the seafloor by emitting sound pulses and recording the back-scattered echoes. Each emitted pulse ensonifies a strip of seafloor whose long axis is perpendicular to the vehicle track. A portion of the pulse energy scatters back in the direction of the sonar instrument; echoes from farther away take longer to reach the sensor and, over time, strips can be assembled to produce the sonar image (Murton et al., 1992). The side-scan sonar has a 6 km swath width and can potentially detect features as small as 2 m across (Masson and Millard, 1991). In practice, beam spreading means along-track resolution is 20–50 m. The data are processed, geometrically corrected and projected in Mercator (Bortoluzzi et al., 1999). Fig. 2 shows the TOBI imagery and its location with respect to the Azores islands. Section 3.2 shows how the nature of the sonograph was used to classify edifices. Interpretation is obviously subjective and can be complicated by the presence of artefacts in the images that result from noise, speckle, interference, change of attitude in the towfish, foreshortening, layover and near-nadir geometry. Previous studies of the seafloor morphology using TOBI and guidelines on interpreting sonar imagery (Blondel and Murton, 1997) were used to aid classification.

High-resolution bathymetry is calculated with TOBI by resolving the angle at which a received sound signal travels between the seafloor and the instrument. This is achieved by measuring the difference in electrical phase of the signal detected on physically separated hydrophones (Flewellen et al., 1994; Escartin et al., 1996). These phase data were processed at sea, and merged with pressure depth and navigation to produce bathymetry. The following morphometric analysis used a bathymetry grid combining these phase data with other coarser-scale bathymetry (obtained from single-beam sounding data obtained from the National Geophysical Data Centre, Boulder Colorado. Sampling rate, accuracy and spatial resolution vary across the region; thus there can be problems in attempting to quantify uncertainty and error. Because of the need to spatially filter the phase bathymetry data, its spatial resolution is not as high as the side-scan imagery and is ~100 m based on the visual appearance of features. The vertical precision of the starboard side data is around 10 m based on observable features in the data, but the port side measurements were noisy , resulting in lower

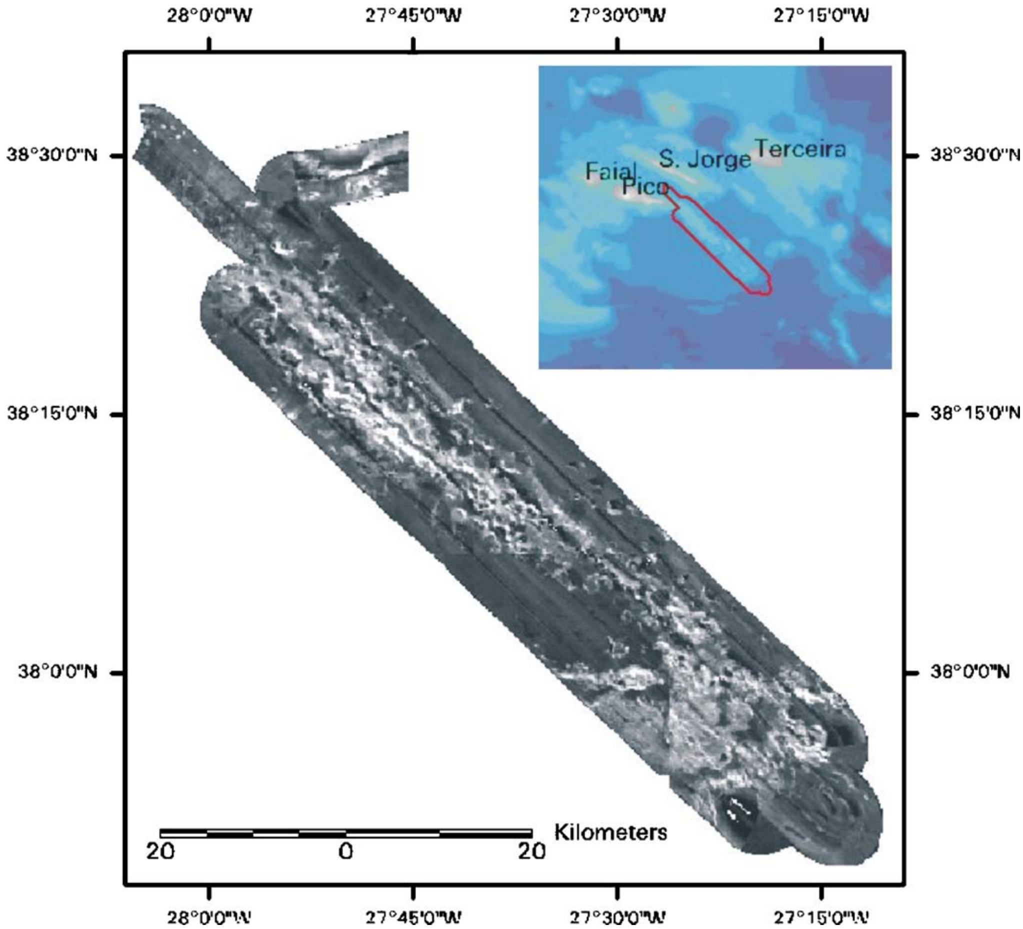

Fig. 2. TOBI imagery and its location in relation to the Azores Plateau. The insert shows the location of the imagery within Fig. 1.

quality port data (Bortoluzzi et al., 1999). A SIR-C (Spacebourne Imaging Radar Band C) image of Pico Island was obtained for analysis from the NASA Jet Propulsion Laboratory, Pasadena.

3.2. Method of analysis

An ArcView 3.2 GIS system, running Imagine Image Support, Spatial Analyst and 3-D Analyst extensions and the downloaded extension bearing.avx were used to examine the sonar images and identify the associated volcanic and tectonic features. Initially, features were classified using the side-scan sonar imagery, with identification of the edifice based on the nature of the backscatter. Guided by studies of the morphology of other mid-ocean ridges which have used TOBI and a preliminary pilot study of the sonographs, the following features were classified:

(1) Cones (Fig. 3a,b): topographic highs with a domed vertical profile, circular or oval in plan view, with high backscatter (shown as white on the sonographs) distinct from the surroundings on the side facing the sonar and a shadow on the other; the shape of the shadow reflecting the cone's profile (Kong et al., 1988). The boundary of the feature was drawn to represent the base contour interpreted from a distinct change in backscatter suggesting a marked change of slope. If one side of the cone is in shadow, its boundary is drawn as symmetrical to the curve of the bright side. No stipulation was made with regard to height, as previous studies used defining heights from 50 m (Magde and Smith, 1995) to 1000 m (Jordan et al., 1983; Batiza et al., 1989) and the reliability of the bathymetry may be a constraining factor, yet the shadow can be more obvious in identifying cones in the imagery. It could be argued that cones with heights of just a few meters may just be local rises in the flow. The texture of cones is judged to be smooth or hummocky, based on the distinction made by Magde and Smith (1995), with hummocky cones defined as those having a bulbous appearance on the cone surface on a scale of tens of meters.

(2) Faults (Fig. 3c): linear branching features which appear on the image as bright or dark lines with consistent shading. The trace of the fault is drawn along the crest.

(3) Volcanic terraces (Fig. 3d): display a hummocky texture, with bright, curved, striping giving a stepped appearance.

(4) Hummocky flows (Fig. 3e): bulbous mottled appearance on sonograph believed to be associated with pillow lava flows. They are distinguished from cones as they are not an isolated feature, and are not as high and therefore, without a distinctive shadow.

Areas of pelagic sediment appear matte grey on sonographs. Some features are not classified due to ambiguity in interpretation.

The boundaries of each edifice were delineated using the annotation tool in ArcView, and the classification was confirmed by an analysis of the bathymetric data. The five bathymetric data sets were combined in ArcView, and the co-ordinates converted using ERDAS co-ordinate converter and ArcInfo to correspond to the images. The interpolate grid tool in 3d-Analyst was used to make a Digital Elevation Model of Pico Ridge, with the cell grid output size set to 10 m. The images and polygon themes of each edifice were overlaid onto the bathymetry to obtain a 3D view of the ridge.

The measurement tool in ArcView was used to measure several parameters. Measurements were taken along-track where possible to reduce the effect of slant-range distortions. All measurements were made at least three times and the median value taken. Parameters measured include the area and perimeter of the feature (these are calculated automatically using the ArcView field editor) and orientation which was calculated from the most northerly to the most southerly point using the bearing extension. The information tool is used to obtain spot heights from a DEM of the ridge with the themes and imagery overlaid. The diameter of cones is calculated using the automatically measured perimeter divided by π. Cones also had their along-track diameters measured manually using the measuring tool, parallel to the direction of the vehicle track at the cone's peak, in case the calculated diameter was not representative of the diameter of an elongated feature. The across-track diameter of the cones was measured manually in order to calculate the aspect ratio of the cone (along-track divided by across-track diameter). The maximum diameter was measured if the major axis was oblique to the vehicle track.

The plan shape of seamounts (whether circular or elongate; Ruiz et al., 2000) was noted, and the azimuth of any elongated cones was measured using the bearing tool in ArcView along with the maximum length of elongation and whether elongation was along-track, across-track or oblique to the vehicle track. The nature of the cone's profile, whether peaked or flat, was also noted (the shape of the shadow being a good indicator). For seamounts that

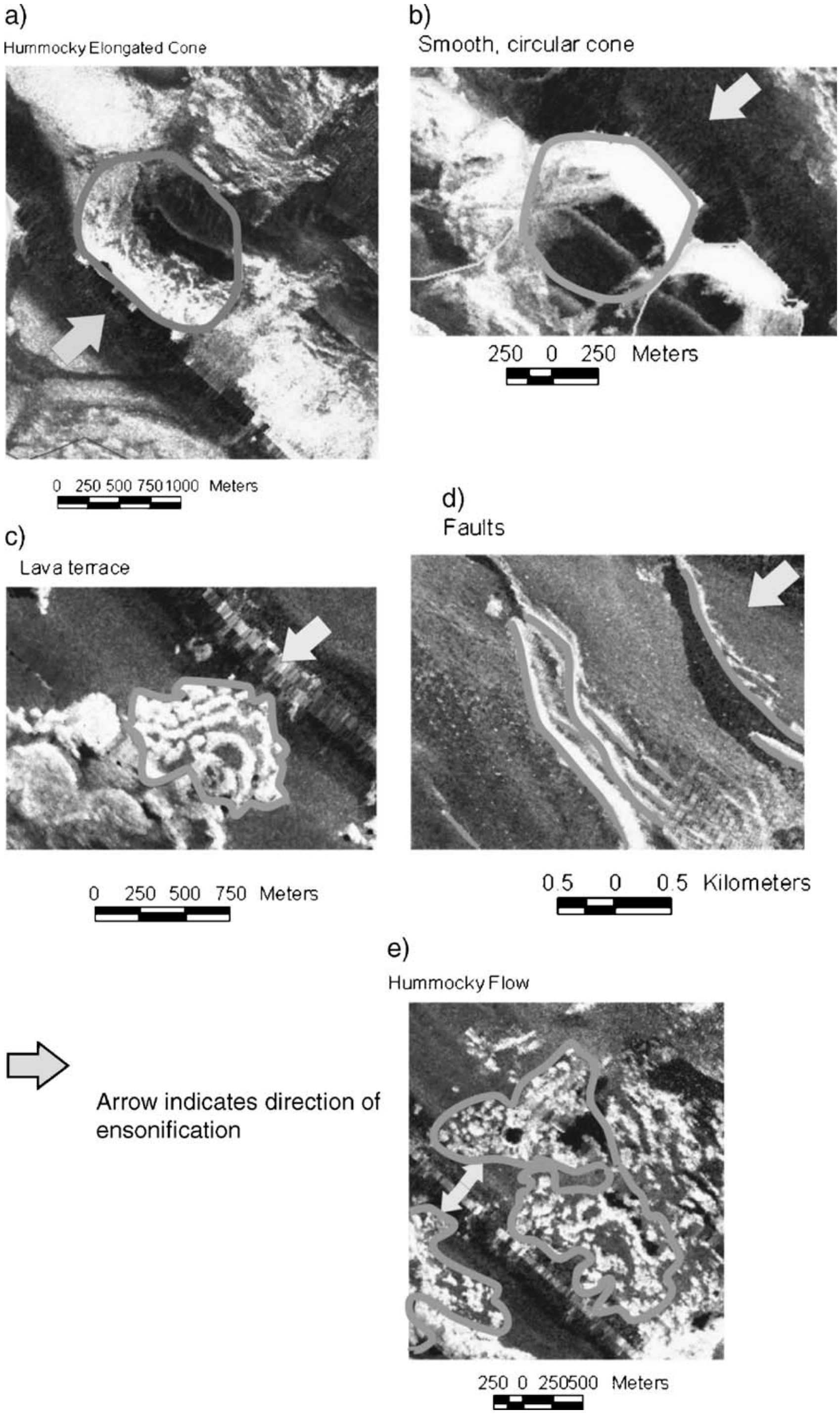

Fig. 3. Examples of the features classified as: (a) hummocky cones; (b) smooth cones; (c) terraces; (d) faults; (e) hummocky flows. Areas of high backscatter are shown in white.

have a flat rather than a peaked summit, flatness can be calculated by dividing the summit radius by the basal radius (Smith, 1988; Magde and Smith, 1995; Scheirer and Macdonald, 1995; Rabain et al., 2001). An index of the profile of the cone was calculated by dividing the height by the basal diameter (Clague et

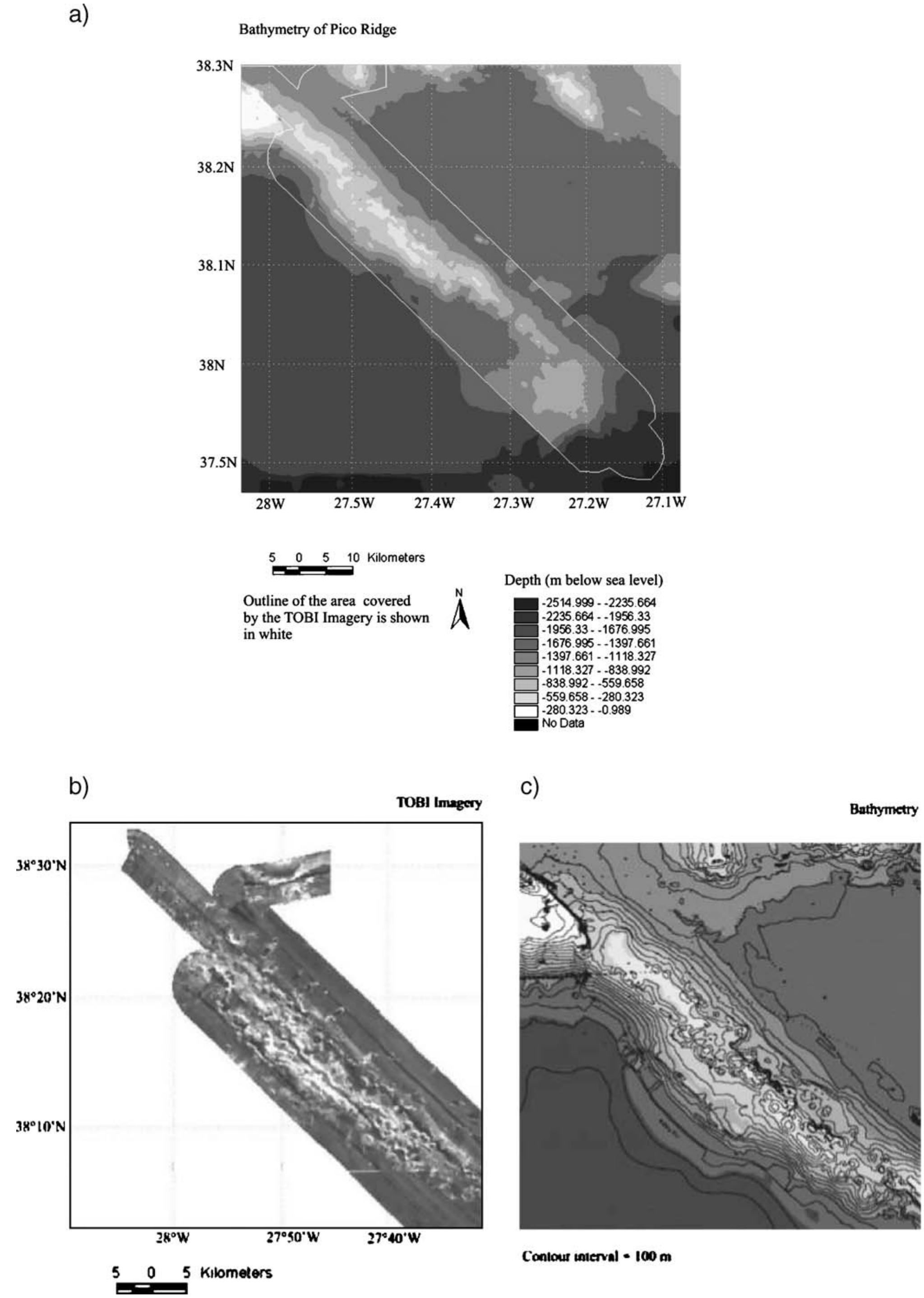

Fig. 4. Classified TOBI imagery of Pico submarine ridge: (a) the bathymetry of Pico ridge; (b) TOBI imagery of the northwest “upper” section of Pico ridge; (c) bathymetry of the northwest section of Pico Ridge; (d) TOBI imagery of the southeast “lower” section of Pico ridge; (e) bathymetry of the southeast section of Pico ridge; (f) mapping Pico Ridge: a simplified interpretation of the morphology of the north west section of Pico ridge using the imagery and bathymetric data; (g) mapping Pico Ridge: a simplified interpretation of the morphology of the south east section of Pico ridge using the imagery and bathymetric data.

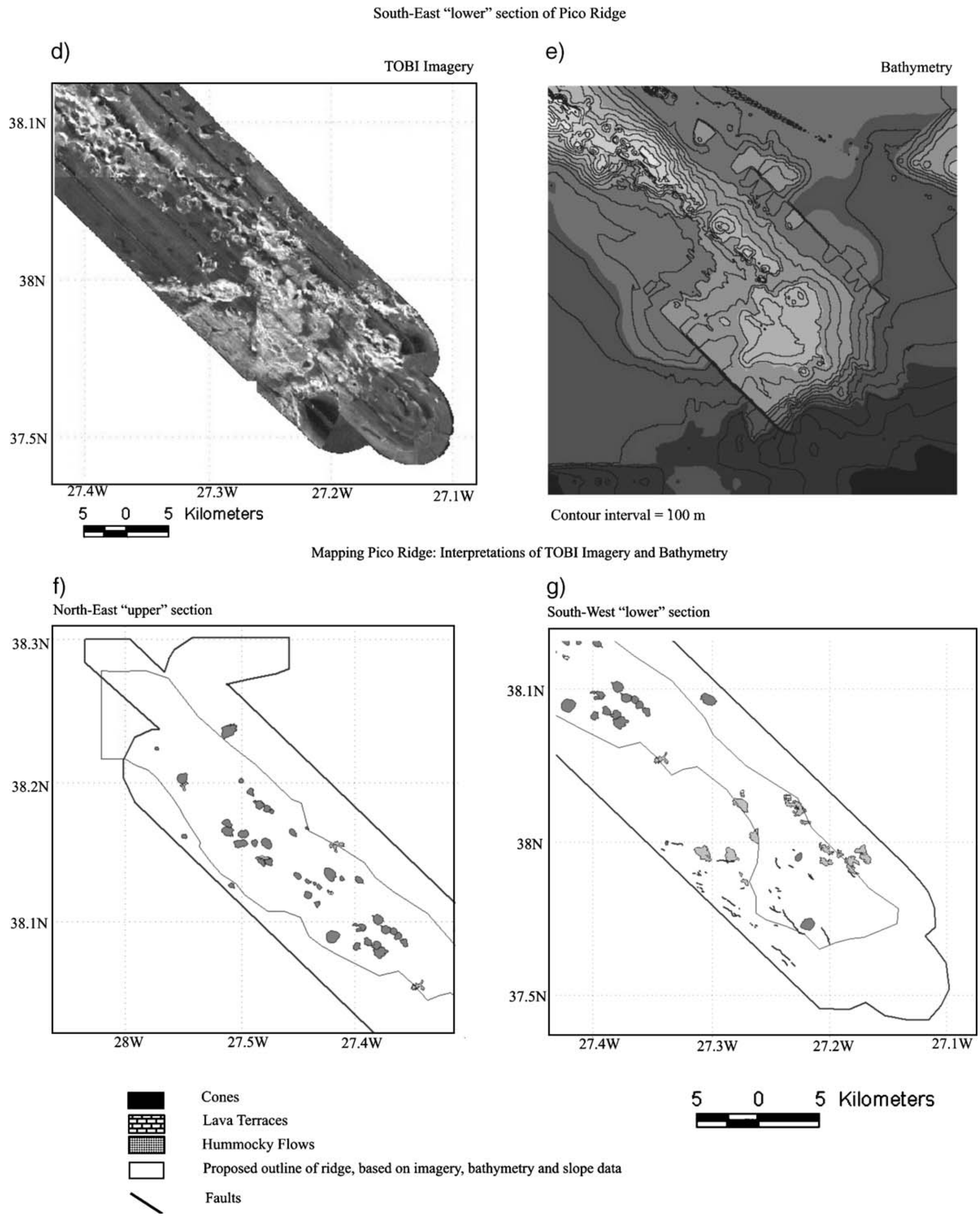

Fig. 4 (*continued*).

al., 2000) and the volume of cones was calculated using the formula:

$$\pi r^2 h/3 \quad (1)$$

where r is cone radius and h is cone height

Shadow length was measured and used to calculate cone height by measuring the depth and height of TOBI and the distance from nadir to the peak of the cone and the principle of similar triangles (Blondel and Murton, 1997). Slope angle for individual cones was calculated from (Smith, 1988; Rabain et al., 2001):

$$\text{Slope angle} \quad (\varepsilon) = \tan^{-1}(h/r) \tag{2}$$

where h is cone height and r is the radius of the cone (taken as half of the calculated diameter).

Slopes over larger areas of the ridge were calculated using the interpolate-slope tool in ArcView.

The different dimensions of cones were plotted against each other (Smith, 1988; Smith and Jordan, 1988) to examine whether features display self similarity i.e. maintaining a uniform ratio of diameter/height. Mann–Whitney U tests were performed to see if there is a statistically significant difference between the dimensions of hummocky and smooth cone populations and circular and elongate cone populations. Statistical tests were performed on the dimensions of cones in order to aid inference of the eruptive processes involved in the evolution of the ridge. The distribution of cones was analysed by performing a nearest-neighbour analysis which involves measuring the distance between each cone and the one nearest to it and then applying the nearest-neighbour formula:

$$\text{Nearest-neighbour index} = d_{\text{obs}}/d_{\text{ran}} \tag{3}$$

where d_{obs} is observed mean nearest-neighbour distance, d_{ran} is the expected nearest-neighbour distance calculated from:

$$1/2\sqrt{p} \tag{4}$$

where p is the density of points.

The nearest-neighbour index then gives an indication of whether the cones are randomly distributed or clustered, which enables an assessment of the likelihood of cones being monogenetic and being formed over a single magma reservoir. The significance of the test can be checked by comparing a C value with values in statistical tables (Ebdon, 1985):

$$C \text{ value for NNI significance}: \quad d_{\text{obs}} - d_{\text{ran}}/0.26136\sqrt{(np)} \tag{5}$$

where n is the number of points and p is the spatial density of points.

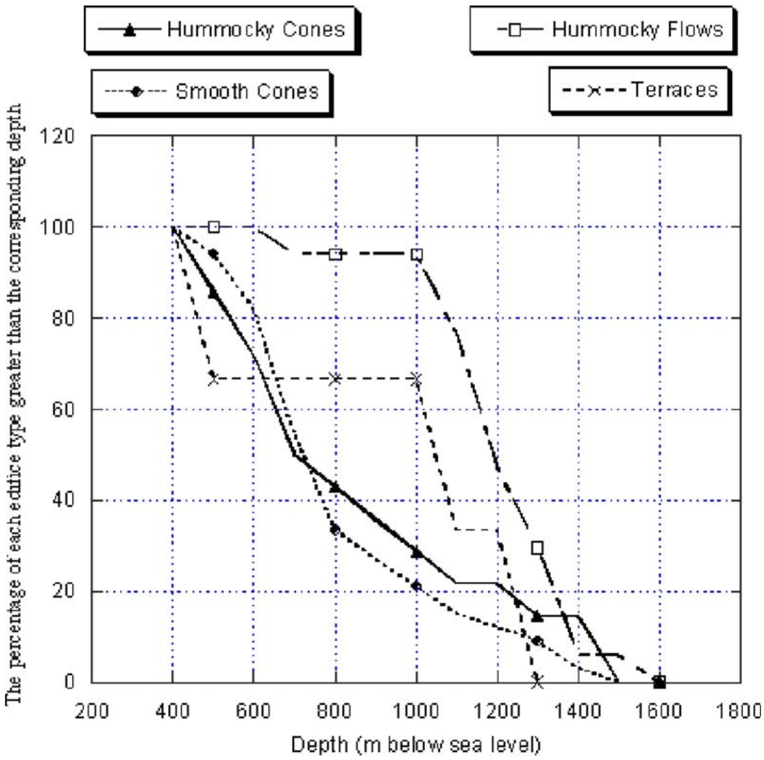

Fig. 5. Cumulative plot showing the distribution of edifice type by depth, as a percentage of each edifice population greater than a certain depth.

The two-point-azimuth method is another test for evaluating whether the alignments in a set of points are random. Azimuths between the peaks of the cones and all other cones in the field are measured. The azimuths are assigned to eighteen 10° bins and peaks in the distribution are analysed. If the distribution of the points is random, the azimuths will not show any preferred direction (Wadge and Cross, 1988).

4. Results and analysis

The Pico submarine volcanic ridge extends south-east from Pico Island on a bearing of N131°E. It is approximately 83 km long and 9.6 km wide. There is a 4.1-km-long break in the continuity of the ridge, approximately 47 km south-east of Pico. The data on the depth and altitude of TOBI show that the deepest part of the ridge is 2.5 km below sea level at its farthest extent from the island (Fig. 4a). Arcview shows that the flanks of Pico Ridge have slopes of 9° – 19°, and contours suggest that gradients are up to 160 m/km, with a long-axis gradient of ∼10–15 m/km. The long-axis topography is undulating rather than gradually sloping and the ridge has an angular shape in cross-section, with steep sides. The ridge is not symmetrical about the long axis. Areas away from the ridge are covered with pelagic sediment, but the ridge itself has cones, hummocky flows and lava terraces along the main body of the ridge. 47 cones have been classified on the Pico submarine ridge; there are also 3 sets of lava terraces and 17 areas of hummocky lava flows. Fig. 4b, c, d and e show the TOBI imagery and the bathymetry split into an upper north-west and lower south-east section respectively. Fig. 4f and g are then interpretations of the morphology of the ridge in each section from an analysis of the imagery and the bathymetric data.

The different types of volcanic landform – smooth cone, hummocky cone, hummocky flow and lava terrace – are not confined to different specific depth ranges, suggesting ambient sea water pressure is not a factor determining the nature of the edifice formed. A larger percentage of hummocky flows and terraces are found at greater depths below sea level as shown in Fig. 5. Cones occur at depths ranging from 322 m to 1545 m below sea level. Hummocky flows are found within a range of depths from 732 m to 1547 m below sea level. There is no correlation between the depth of a flow and its surface area. The three sets of terraces, with heights of 88 m, 97 and 232 m, consist of three steps and are evident at a range of depths from 369 m to 1391 m below sea level.

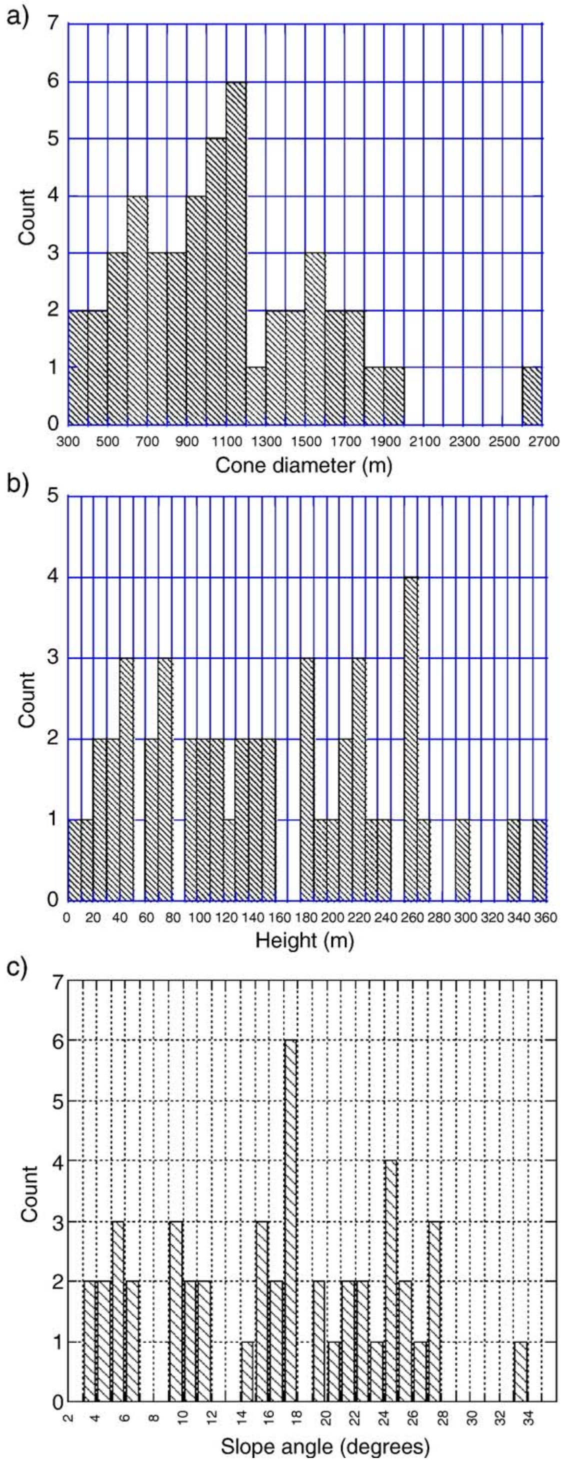

Fig. 6. Histograms of cone dimensions: (a) histogram of cone diameter; (b) histogram of cone height (omitting one height at 750 m); (c) histogram of the slope angle of the cones.

Cones have a peaked profile rather than a flat top and there is no clear evidence of two distinct cone populations with differing profiles. Diameters range from 304 m to 2695 m. Diameters measured manually rather than calculated automatically can differ by several hundred meters, especially where the cone is elongated in plan form, although when plotted against each other they show a strong positive correlation. The differences are a result of the subjectivity involved in measuring the distances manually and the nature of the algorithms used to calculate the diameter from the perimeter of the cone. The mean diameter of cones using the measured diameters is 948 m (S.D. = 373) and the mean diameter of the cones using the calculated diameters is 1085 m (S.D. = 480). Fig. 6a shows the distribution of the diameters of the cone population; there is a slight modal class at 1100–1200 m but the kurtosis of the data set is low. Heights range from 0.3 m to 750 m, but the height data show a low kurtosis and skew value. The mean height of the cones is 152 m (S.D. = 94), with 57% of cones less than 160 m in height (Fig. 6b). 76% of cones have a profile index of less than 0.2; the range of the profile index is from 0.02 to 0.32 with a mean value of 0.14. The mean slope angle of the cones is 15.6° (S.D. = 7.9°). Slope angles of 2.2° to 32.4° are evident, with a modal class between 16–17°, although the data display a low kurtosis (Fig. 6c).

As Fig. 7 shows, there is only a very weak positive correlation between diameter of the cones, whether measured or calculated, and cone height. Even when data are omitted in cases where the bathymetry is less reliable, the change in diameter can only explain a maximum of 37% of the change in height. If cones with heights less than 10 m are excluded from the calculations – under the premise that topographic highs less than 10 m on pillow lavas may be tumuli rather than cones (Walker, 1991) – there is still only a similarly weak positive correlation between cone diameter and height. The shadow length was also used to calculate cone height using the geometry of the ensonifying system without using the bathymetric data sets. However, there was no relationship between cone diameter and height inferred from shadow length. There is also no relationship evident between the depth of the base of the cone and its height (Fig. 8).

33 of the cones are smooth and 14 have a hummocky texture. There is no obvious spatial distribution related to the differing textures; both types are inter-

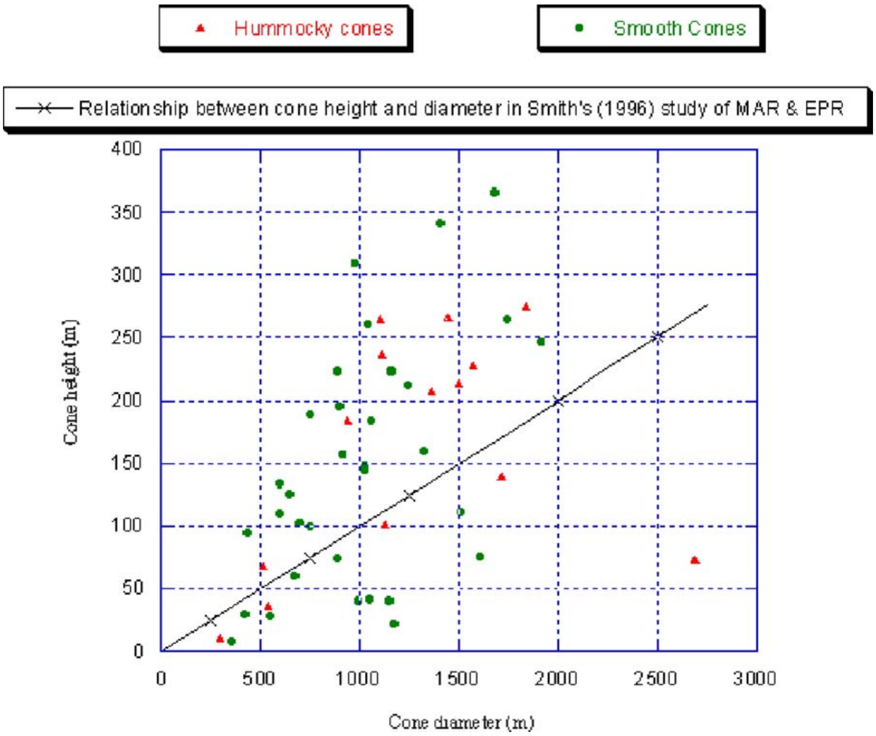

Fig. 7. Plot showing the relationship between cone diameter and height for cones on Pico Ridge, showing the distinction between the smooth and hummocky cone population and a comparison to the ratio between cone diameter and height found by Smith (1996).

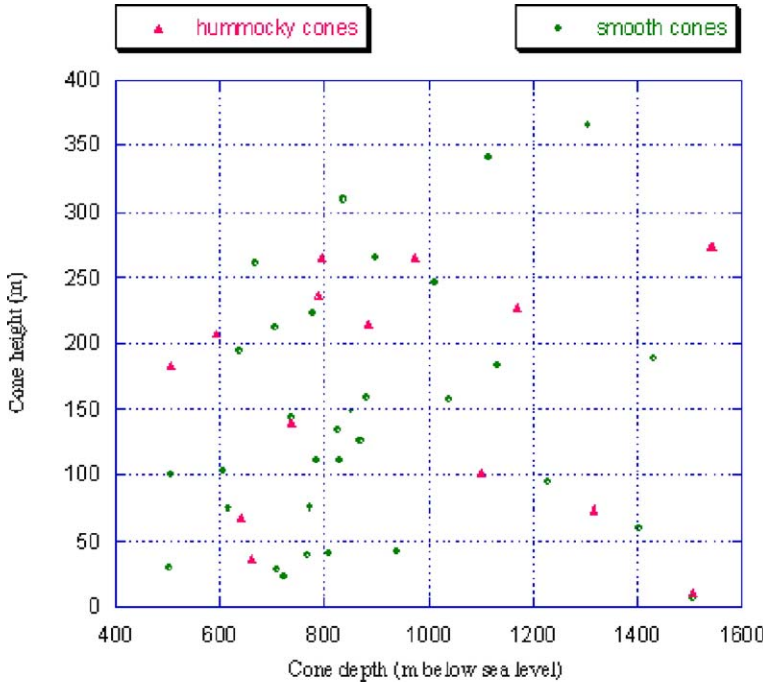

Fig. 8. Plot showing the relationship between eruption depth and cone height for cones on Pico Ridge, showing the distinction between hummocky and smooth cone populations.

mingled, and there is no relationship evident with plan of the cone or location on the ridge axis. Mann–Whitney *U* tests assess the differences in dimensions between the two populations of cones, to further evaluate the possible nature of the eruptive activity producing the edifice. There was no significant difference found between the mean heights of the cones with a hummocky and smooth texture (Fig. 7) and no difference between the mean depths of the cones with a hummocky and smooth texture (Fig. 8). No significant difference was found between the mean slope angle of the hummocky and smooth cone populations. However, a statistically significant difference in the mean measured, but not calculated, diameters of the smooth-cone population and the hummocky-cone population is evident. Using measured diameters, the mean diameter of the hummocky-cone population is 1143 m, the mean diameter of the smooth-cone population is 865 m.

31 cones are elongate in plan form and 16 are circular. The mean direction of elongation has a bearing of 111°N, oblique to the ridge axis. No significant difference was found in the mean diameters between the circular- and elongate-cone populations or the mean heights of the circular- and elongate-cone populations, although there is more scatter in the height of the elongate- than the circular-cone population. Fig. 9a, a cumulative histogram of the diameters of the cones, shows that the population lacks an exponential distribution.

A nearest-neighbour analysis of the cones of the submarine Pico Ridge produced a nearest-neighbour index of 0.86; an index of 1.0 is a random distribution, 0 is a clustered distribution and 2 is a dispersed pattern. A

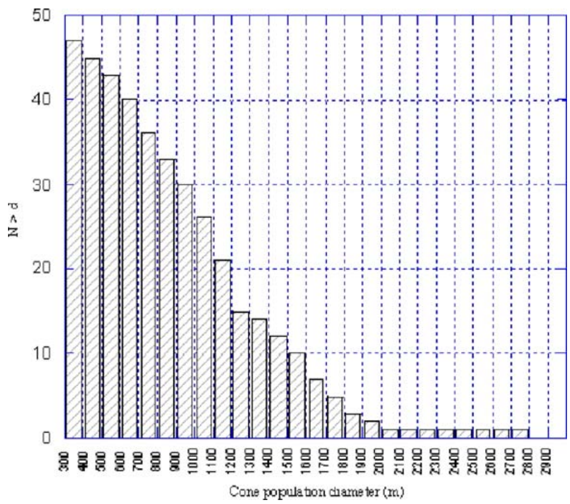

Fig. 9. Cumulative histogram of the diameters of the cone population of Pico Ridge.

comparison of the calculated index against value tables (Ebdon, 1985) shows that the calculated value of the index is greater than the critical level at the 95% significance level, therefore it is not possible to reject the null hypothesis that the distribution of cones is random.

The subaerial volcanic cones identified on the radar image of Pico Island (Fig. 10), have mean diameters of 319 m (S.D. = 116), excluding Mt Pico, and there is a distinct modal class at 250–300 m diameter. A Mann–Whitney *U* test demonstrates that there is a significant statistical difference in the mean diameter of the Pico subaerial and Pico submarine cone populations at the 95% significance level. The nearest-neighbour index for the subaerial cone population is 1.99. In this case, it is possible to reject the null hypothesis at the 95%

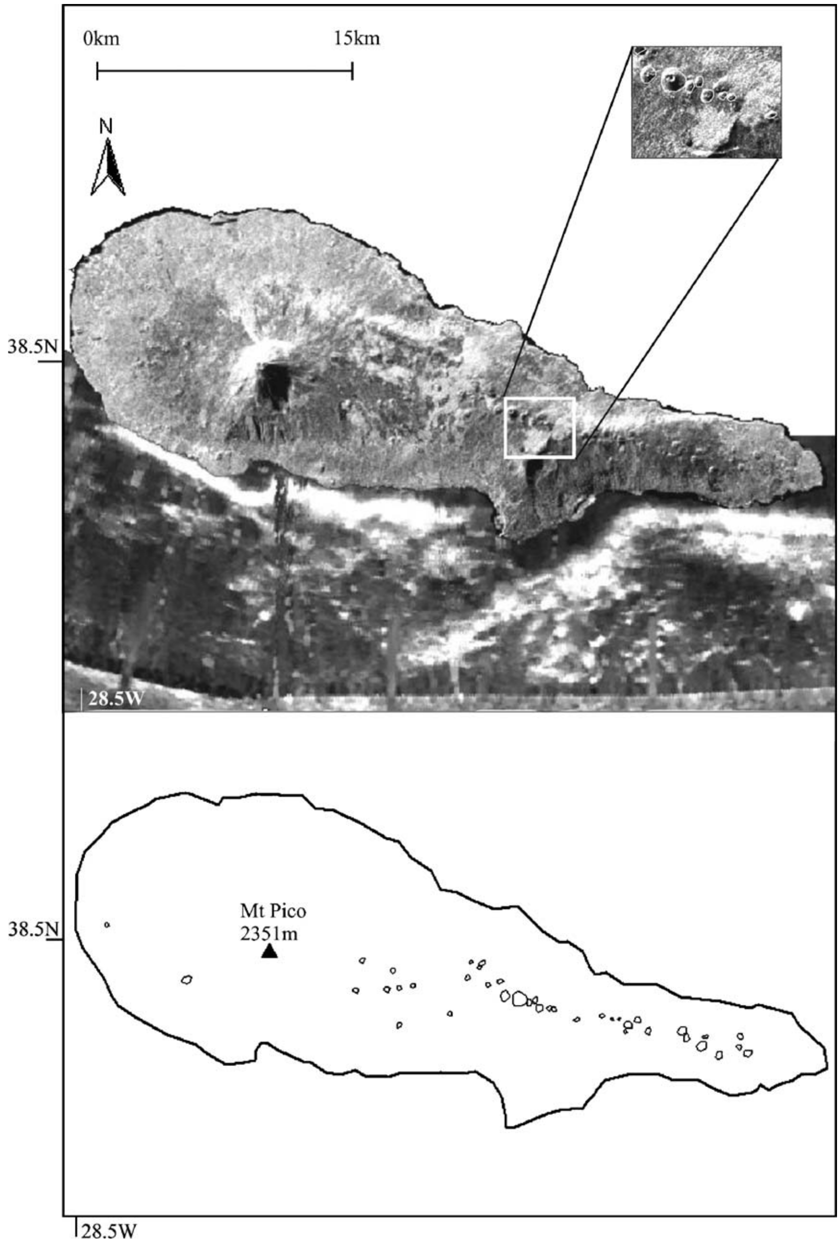

Fig. 10. SIR-C image of Pico Island, showing the declination of cones. Image courtesy of the NASA Jet Propulsion Laboratory. Areas of higher backscatter are indicated by lighter-coloured areas on the sonograph. GLORIA Imagery (Mitchell, 2003) has been mosaicked on the southern side of the island.

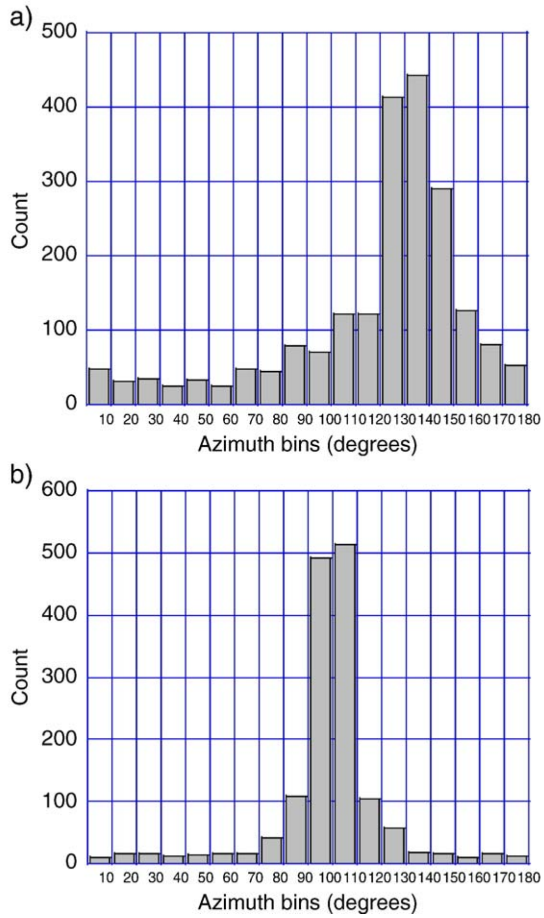

Fig. 11. Histogram showing the results of the two-point-azimuth test on (a) the submarine-cone population and (b) the subaerial-cone population.

significance level, that the distribution of cones on Pico Island is random.

The two-point-azimuth method results show peaks in the azimuth bins of 90°–110° for the subaerial cone population (68% of the azimuths are within 90°–110° bins). Peaks are evident in the 120°–140° azimuth bins for the submarine cone population (40% of the azimuths are within this range). The azimuths do display a preferred direction (Fig. 11a and b) suggesting the distribution of the cones is not random.

5. Discussion

5.1. Surface texture and inferred eruption mechanisms

It is commonly assumed that hummocky flows are associated with pillow lavas produced by effusive less fluid (high viscosity) and less voluminous eruptions; smooth lava flows are produced by eruptions of more fluid lava with a much higher eruption rate (Griffiths and Fink, 1992, 1993; Gregg and Fink, 1995; Kennish and Lutz, 1998; Batiza and White, 2000). However, it should be noted that the resolution of TOBI imagery is not high enough to determine if individual lava flows are smooth sheets or pillow flows, only an overall indication of textures is given. Analogue experiments address lava texture on the scales of meters, whereas TOBI imagery gives an indication of morphology at a grosser scale. Submersible dives and photographs have demonstrated that pillow lavas can be assigned to areas, which display a smooth texture on sonographs (Bryan et al., 1994; Smith et al., 2002).

Behn et al.'s (2004) study of the Galapagos Spreading Centre suggests that eruption rate is the primary control on lava texture. The majority of cones on the Pico Ridge have a smooth texture. The presence of both textures is indicative of both high and low eruption rates, suggesting magma supply to the ridge has varied over time. The majority of cones studied in sections of the Mid-Atlantic Ridge (Smith et al., 1995a) are hummocky rather than smooth. The Azores Plateau is a hotspot, a region of hypothesized magma upwelling; the associated thinner lithosphere and increased magma supply imply a higher eruption rate, hence the predominance of the smooth texture. Similarly, the percentage of smooth seamounts increases nearer the hotspot at the Reykjanes Ridge and in areas which have an increased magma supply due to an increase in partial melting (Magde and Smith, 1995).

The Mann–Whitney U test showed that there was no significant difference between the mean depths of cones for the smooth and the hummocky cone population; hence the overlying water pressure does not appear to have an affect on the nature of the eruption. Laboratory studies (Griffiths and Fink, 1992) suggest that the chemistry of the lava has little control on the texture of lava flows: pillow lavas were produced as crustal growth rates were increased and/or effusion rate and slope was decreased (Kennish and Lutz, 1998). These analogue experiments and the lack of relationship between texture and depth suggest there are additional controls on texture at Pico apart from geochemistry and eruption depth. Volatile content (especially proportions of water and carbon dioxide) may affect the style of eruption and lava texture. Exsolution of water would be expected to decrease as depth and the confining pressure increase, but no relationship was found between sonar texture and depth in the range of depths studied. Carbon dioxide exsolves at a much higher pressure however, raising the possibility of explosive gas exsolution occurring to much greater water depths (Hekinian et al., 2000). It might also be possible that the number and nature of the vesicles have an influence via their effects on lava viscosity and yield strength, which in turn could affect the texture of edifices formed (Kennish and Lutz, 1998). There are certain depths of the ridge that are not classified which may affect how representative the results are – unclassified areas are along the shallower ridge crest and appear to have a smooth texture.

Our analysis raises the question as to why hummocky cones have a significantly greater mean diameter than smooth cones, if a smooth texture is thought to reflect a higher eruption rate. It might also be expected that cones with a smooth texture would have a slope angle equal to the angle of repose of the material. However, there is no significant difference between the mean angle of the hummocky cone population and the smooth cone population. This may be because successive eruptions of different styles have occurred through the same vent/dyke and are therefore, contributing to the overall nature of the edifice formed: cones with an outer rough texture could be superimposed onto cones with a previously smooth texture as eruption rates decrease over time. Kennish and Lutz (1998) also suggest that pillow lavas may be formed in later eruptive stages and smooth textures are a result of brief but voluminous flows from fissures. There are striations on the flanks of the cones, which may suggest the presence of gullies as a result of mass movement which would affect slope angles.

5.2. Edifice morphology

All cones were identified as being peaked. The dominance of one profile type, rather than two or more populations with differing profiles, and the lack of correlation between water depth and cone height, suggest that there is one common eruption mechanism. Cones do not develop self-similarly; there is no constant relationship between diameter and cone height. The lack of a linear relationship suggests cones do not develop in a simple way. There does not appear to be a limiting value for the height of cones either. A critical height may not be obvious because the cones are so youthful that a critical height has not yet been reached. However, dredge samples collected from the Azores Plateau by cruises *Poseidon* 232 in 1997 and *Poseidon* 286 in 2002 suggest that the samples are old, over 100,000 years (Karsten Haase, personal communication). This suggests therefore that eruption volumes and pressures have no particular limits.

There are no flat-topped cones evident at Pico. Clague et al. (2000) suggest that flat- topped cones with wide bases in the Hawaiian Islands develop as submarine lava ponds that overflow. According to Clague et al. (2000), these require a certain set of environmental conditions: low volatile content, moderate-high confining pressure, long-lived steady effusive eruption, moderate eruption rates and low slopes. Analogue experiments involving gravity models show that a similar set of environmental conditions – high lava viscosity, gentle regional slope and low effusion rates – is required for the development of lava terraces (Zhu et al., 2002). The lack of flat-topped cones and the smaller, less abundant terraces at Pico, than at Puna Ridge, suggests one or more of the above environmental criteria may not be fulfilled at Pico Ridge. The slopes are low across the majority of the area, but perhaps the volatile content is not low enough, that the eruptions are not long lived; and/or that the eruption rates have been too high (a smooth texture is evident, implying a relatively high eruption rate).

Pico cones are smaller in diameter and height than cones that have been measured near the Pacific Rise (Smith, 1988). Heights of Pacific seamounts are 100 m to hundreds of metres, and this can be attributed to the more abundant magma supply at a fast-spreading ridge. Pico Ridge cones have similar cone heights and diameters of a similar magnitude to cones at the MAR. In a study of the MAR and EPR, Smith et al. (1995b) and Smith (1996) demonstrated that the diameters of seamounts are typically 10 times greater than their heights, a ratio that corresponds within an order of magnitude to the profile indices (height/diameter) of the Pico cone populations. The diameter–height relationship found at the MAR and EPR is much stronger ($r^2 = 0.92$) than the relationship between diameter and height of cones at Pico ridge. As Fig. 7 shows, Pico cones typically have a larger profile index – such that heights are greater or diameters are smaller – than would be expected from Smith's (1996) ratio. At the Mid-Atlantic Ridge the relatively large diameter with respect to cone height, suggests that cones develop preferentially outwards rather than upwards (Smith et al., 1995a). Although this is generally also true of the Pico Ridge, the cone aspect ratio varies with height, so the tendency to spread also changes.

At the Reykjanes Ridge dimensions of cones (Magde and Smith, 1995) are similar to those measured on Pico Ridge and both areas display a relatively large proportion of cones with a smooth texture rather than a hummocky texture, whereas on sections of the MAR, 83% of cones were found to be hummocky (Smith et al., 1995a). Although the lava at the two regions can display marked differences in major- and trace-element constituents (Langmuir et al., 1992), both locations lie over a regional melting anomaly, so the Azores Plateau and Reykjanes Ridge are probably more comparable in terms of magma supply and lithospheric thickness than Azores and the MAR. This suggests that magma supply, and eruption size and frequency largely determine the morphology of cones. However, unlike at Pico, the majority of Reykjanes cones are flat-topped, with flatter cones tending to be larger and smoother; this has been attributed to the magma flux not being a limiting factor (Smith et al., 1995b). Pico cones are also of similar dimensions to the cones associated with Puna Ridge, a 75-km-long submarine extension of the Kilauea East rift zone, Hawai‘i (Smith et al., 2002). However, there appears to be two distinct cone populations at Puna unlike at Pico ridge, with a distinction in morphology seeming to form at a height of 100 m. This has been attributed to differences in the magma supply and plumbing system between the two sets of Puna cones. Pico submarine cones have a greater diameter than Pico subaerial cones, probably because lava in the submarine environment is subject to enhanced cooling and the edifices produced will have a greater mechanical stability, thus able to grow larger in size (Smith and Cann, 1999).

5.3. Geometrical development of the ridge

Regional tectonics influence the development of the ridge: the general trend of the ridge axis is consistent with the tectonic strike of the Azores Plateau. The mean direction of the elongation of cones is 111°N, with a modal class of 100°–140°, which is consistent with the main tectonic strike and fault orientation of the area at 120°N and 150°N (Lourenco et al., 1998; Luis et al., 1998; Miranda et al., 1998). The majority of the elongated cones are elongated oblique to the track; hence, it is unlikely to be due to distortion on the imagery, as that would be along-track. The cones are not elongated down the bathymetric gradient either. The results of the TPA analysis are also consistent with the tectonic alignment of the plateau. There is no significant difference between the mean diameter of the circular-cone population and the elongate-cone population; hence, it seems unlikely that elongation is a stage in the life cycle of cones as they develop. It is possible that elongated cones develop over dykes (Batiza and Vanko, 1983; Lourenco et al., 1998; Davies et al., 2002), which have a linear form, and circular cones are point-source features. It may be expected that the two different types of volcanism would produce cone populations of different size (Behn et al., 2004). However, no significant difference in the mean height or diameter of the circular- and elongate-cone populations was found to exist. Thus, for Pico Ridge, we reject the inference that different magma supplies for different cone shapes account for different cone shapes.

There is evidence of groups of cones, with both smooth and hummocky textures, forming linear arrays along the main trend of the ridge axis (Fig. 4b). This may be a result of cooling of an eruptive fissure, which would be expected to be parallel to the main ridge axis, and the centralization of eruptions to points along it (Head et al., 1996; Behn et al., 2004). Inhibition of gas exsolution and hydrothermal effects decrease the ascent of erupting magma and enhance cooling, which increases magma viscosity, causing a greater tendency to centralise along the widest parts of the dyke. Head et al. (1996) also suggested a relationship between dyke width and the size of the edifices produced; the radii of the cones at Pico Ridge would suggest they are formed from dykes which are between 0.4 and 0.8 m wide, assuming MAR and Azores magma characteristics are comparable.

The random distribution of cones suggested by the nearest-neighbour analysis may reflect eruption from fissures that are arranged randomly; this would still produce preferred azimuths as found in the two point azimuth test. Fissure eruptions would also favour the formation of smooth cones (Behn et al., 2004), as is evident at Pico Ridge. This mechanism for the formation of cones is then explained by successive eruptions from wide dykes rather than shallow subsurface magma reservoirs (Head et al., 1996). This is unlike Reykjanes (Smith et al., 1995a) where clusters of cones have been found that are believed to be related to magma bodies. Smith et al. (1995b) suggested that clusters of cones on the seafloor could mean that mid and lower oceanic crust comprises a multitude of magma bodies of different sizes and levels, with each magma body feeding a distinct monogenetic volcano. This would suggest a complicated crustal structure in which dykes and lavas are inter-fingered in a shallow crust (Smith and Cann, 1992). The Pico subaerial cones do display some clustering, and they may be influenced by the very narrow NW–SE linear nature of the island and the main fissure along it, which is consistent with the tectonic strike of the area (Woodhall, 1974; Mitchell et al., 2003a). The spread of Pico submarine-cone azimuths is greater than the spread of subaerial cone azimuths. This is possibly because the area of dyke intrusion migrates laterally over time. In the subaerial setting, erupted flows bury older cones, leaving the cone distribution reflecting the more recent episodes of volcanic rifting and eruption. In the submarine setting, individual flows are less widespread, so they are less likely to bury older cones and the resulting cone distribution represents a longer time period of volcanism. These effects are further enhanced by the different rates of subaerial and submarine erosion (Mitchell et al., 2003b), which are likely to lead to preferential removal of the subaerial cones.

As an alternative to cones being fissure-fed or directly fed by magma bodies, a lava tube system (Gregg and Fornari, 1998) may exist at some submarine ridges and a lava-tube-fed origin has been invoked for the Puna Ridge, Hawai'i (Smith and Cann, 1999). In Smith and Cann's revised model of the crustal construction at ocean ridges, most dykes are emplaced in a narrow zone beneath the median valley floor. Lavas are erupted above this zone and are transported in lava tubes. This implies a crustal structure in which lavas overlies sheeted dykes with an abrupt transition between the zones. The lava tubes have been shown to be sufficiently thermally and mechanically stable to transport lava down the flanks of the volcanic ridge and create the morphology of the features on the valley floor (Smith and Cann, 1999). The morphology of Puna Ridge was interpreted to be a result of two fissure vents on the ridge crest overlying the axis of dyke intrusion producing primary features, with central vent eruptions dominating downcrest and lava tubes feeding secondary features such as cones and terraces (Smith et al., 2002). Lava tubes are also significant in the construction of the subaerial volcanic ridge at Kilauea (Leslie et al., 2004).

The volcanic cones and terraces associated with Pico Ridge are of the same size or smaller than those along the Puna Ridge and occur at similar depths. However, the contour patterns at Pico and the distribution of the edifices suggest that the presence of lava tubes is unlikely; outer cones cannot obviously be fed from the central axis as there is no suitable down-slope bathymetric pathway. Such a gradient is required to provide the magmatic pressure gradient and reduce exsolution of volatiles, maintaining an effusive eruption and it would be difficult to explain how an up-gradient tube path as required by some of the cone locations on Pico, could become established and stable. Hummocky cones would also be more prevalent if they were secondary features fed by lava tubes as at Puna Ridge. The majority of features are therefore likely to be primary features (Smith and Cann, 1999), probably fed directly by fissures. The ridge seems to be predominantly formed from fissure eruptions with little transport of lava down its flanks.

It is possible that the volcanic terraces were fed by a lava tube network. Radial-flow forms at the distal end of a tube and inflation from within causes development of the terrace. This results in growth that is first upward then outward (Kennish and Lutz, 1998; Smith and Cann, 1999; Smith et al., 2002). The three sets of terraces are located on the periphery of the main ridge axis and would therefore permit movement of magma down a bathymetric gradient in lava tubes. The terraces at Pico Ridge are smaller than the ones found at Hawai'i, which can be several hundred meters high and up to a kilometer in diameter (Smith et al., 2002). The Pico terraces are nearer to the main axis and are not as numerous, which may be a result of the tube system being less well developed.

The majority of features on the ridge are primary features. The location of cones is likely to be due to the distribution of dykes, which is influenced by the regional tectonic trend. Hence, the tectonic framework of the Azores Plateau has a significant influence on the volcanic morphology of Pico Ridge (Lourenco et al., 1998). The WNW–ESE and NNW–SSE pattern of faulting is a result of the deformation across the region which is transtensional. Tectonic stress generated by the spreading controls the local orientation of the axis of least compressive stress. Dykes propagating away from a magma chamber are perpendicular to this. Fissure-fed eruptions are believed to be the dominant process of ridge construction in this region.

6. Conclusions

Cones associated with Pico submarine volcanic ridge display one profile type, and are peaked rather than flat-topped. The cones have a greater profile index than the cones of the MAR, Puna and Reykjanes. However, there is not a strong correlation between diameter and height as has been found to exist at many other ridges. This suggests that cones at Pico Ridge do not evolve in a simple way and that cones do not develop self-similarly. No critical height for cones seems to exist. The majority of cones are elongated and are of a smooth texture. The proximity to the Azores regional mantle-melting anomaly and associated high magma volatile contents are probably responsible for high eruption rates producing smooth flows and are probably a reason for the similarities in cone size and shape to those studied on Reykjanes Ridge, near the Iceland hotspot. Depth does not appear to have a significant control on cone height or texture at Pico Ridge, suggesting a common eruption mechanism. Hummocky cones have a significantly larger mean diameter from the smooth-cone population and this may be a result of successive eruptions, with changes in the eruption rate over time. Submarine cones are distributed randomly, whereas subaerial cones are not and are confined to a smaller range of alignments. This may be because the subaerial cone population is younger as it is censored by subaerial erosion and by over-covering by later flows, whereas the submarine population records a longer geological history of rifting and eruption which has migrated laterally over time. The lack of suitable down-gradient progressive bathymetric pathways suggests that it is unlikely that lava tubes supply the cones around the margins of the ridge. It is possible that the lava terraces are fed by lava tubes. Fissure eruptions seem to be important in crustal magma supply and result in linear arrangements of edifices and elongation of cones consistent with the tectonic strike of the Plateau, with cones forming as a dyke cools and the eruption centralises to points along a fissure.

Acknowledgements

We thank Dr. Clive Oppenheimer, Dept. of Geography, Cambridge for his advice on aspects of physical volcanology, Gabriel Amable and Mike Bithell of the same department for assistance with ArcView GIS. Thanks also go to the scientists and crew of the R/V Urania Cruise AZ99 funded by the Italian CNR, and Marco Ligi at the Istituto di Scienze Marine, Bologna for the development of the bathymetry and the Southampton Oceanography Centre TOBI Group for running the TOBI system with the support of the European Union through a European Access to the Seafloor Survey Systems grant. We appreciate the assistance of George Whitesides, formerly of the Department of Geography at the University of Cambridge who carried out a pilot study that formed the basic motivation for this project. We thank also Dr. Karsten Haase, University of Kiel, for providing information on the results of analysis performed on dredge samples from the Azores. Neil Mitchell was funded by a University Research Fellowship of the Royal Society.

References

Batiza, R., Vanko, D., 1983. Volcanic development of small oceanic central volcanoes on the flanks of the East Pacific Rise inferred from narrow beam echo-sounder surveys. Marine Geology 54, 53–90.

Batiza, R., White, J.D.L., 2000. Submarine lavas and hyaloclastite. In: Sigurdsson, H., Houghton, B., McNutt, S.R., Rymer, H., Stix, J. (Eds.), Encyclopedia of Volcanoes. Academic Press, San Diego, CA, pp. 361–381.

Batiza, R., Fox, P.J., Vogt, P.R., Cande, S.C., Grindlay, N.R., Melson, W.G., O'Hearn, T., 1989. Morphology, abundance and chemistry of near-ridge seamounts in the vicinity of the Mid-Atlantic Ridge ~26°S. Journal of Geology 97, 209–220.

Behn, M.D., Sinton, J.M, Detrick, R.S., 2004. Effect of the Galapagos hotspot on sea floor volcanism along the Galapagos spreading centre (90.0–97.6W). Earth and Planetary Science Letters 217, 331–347.

Bicknell, J.D., Sempere, J.C., Macdonald, K.C., Fox, P.J., 1987. Tectonics of a fast spreading centre: a deep-tow and Sea-Beam survey on the East Pacific Rise at 19°. Marine Geophysical Researches 9, 25–45.

Blondel, P., Murton, B.J., 1997. Handbook of Seafloor Sonar Imagery. John Wiley and Sons, Chichester.

Bortoluzzi, G., Carrara, G., Gamberi, F., Marani, M., Ligi, M., Peniteni, D., Portaro, R., Centorami, G., Rovere, M., Mitchell, N., Jacobs, C., Rouse, I., Flewellen, C., Whittle, S., Luis, J.F., Lourenco, N., Terrinha, P., 1999. Tectonic and pressure controls on the growth of giant volcanic ridges in the Azores region (Atlantic Ocean)Report on TOBI Side-Scan Sonar, Swath Bathymetry, SBP Profiling, and Magnetic Investigations During Cruise AZ99. Istituto per la Geologia Marina – CNR Bologna Technical Report, vol. 53.

Briais, A., Sloan, H., Parson, L.M., Murton, B.J., 2000. Accretionary processes in the axial valley of the Mid-Atlantic Ridge 27°N–30°N from TOBI side-scan sonar images. Marine Geophysical Researches 21 (1/2), 87–119.

Bryan, W.B., Humprhis, S.E., Thompson, B., Casey, J., 1994. Comparative volcanology of small axial eruptive centres in the MARK area. Journal of Geophysical Research 99, 2973–2984.

Cannat, M., Briais, A., Deplus, C., Escartin, J., Georgen, J., Lin, J., Mercouriev, S., Meyzen, C., Muller, M., Pouliquen, G., Rabain, A., da Silva, P., 1999. Mid-Atlantic Ridge–Azores hotspot interactions: along-axis migration of a hotspot-derived event of enhanced magmatism 10 to 4 Ma ago. Earth and Planetary Science Letters 173 (3), 257–269.

Clague, D.A., Moore, J.G., Reynolds, J.R., 2000. Formation of flat-topped volcanic cones in Hawai'i. Bulletin of Volcanology 62, 214–233.

Cowie, P.A., Malinverno, A., Ryan, W.B.F., Edwards, M.H., 1994. Quantitative fault studies on the East Pacific Rise: a comparison of sonar imaging techniques. Journal of Geophysical Research 99 (B8), 15205–15218.

Critchley, M.F., Coller, D.W., German, C.R., Blondel, P., Flewellen, C., Parson, L., Rouse, I., Teare, D., Bougault, H., Needham, D., Miranda, M., 1994. Integration of deep tow side-scan sonar imagery, bathymetry and other data along the Mid-Atlantic Ridge. EOS Transactions of the American Geophysical Union, Fall Meeting, p. 579.

Davies, R., Bell, B.R., Cartwright, J.A., Shoulders, S., 2002. Three-dimensional seismic imaging of Paleogene dike-fed submarine volcanoes from the northeast Atlantic margin. Geology 30 (3), 223–226.

Ebdon, D., 1985. Statistics in Geography, Second edition. Blackwell Publishers Ltd., Oxford.

Edwards, M.H., Fornari, D.J., Malinverno, A., Ryan, W.B.F., Madsen, J., 1991. The regional tectonic fabric of the East Pacific Rise from 12°50′N to 15°10′N. Journal of Geophysical Research 96 (B5), 7995–8017.

Escartin, J., Slootweg, A.P., Flewelen, C.G., Rouse, I.A., Searle, R.C., Mitchell, N.C., Cowie, P.A., Allerton, S., MacLeoad, C.J., Russell, S.M., Tanaka, T., 1996. The first TOBI swath bathymetry. BRIDGE Newsletter 11, 28–29.

Escartin, J., Cannat, M., Pouliquen, G., Rabain, A., 2001. Crustal thickness of V-shaped ridges south of the Azores: interaction of the Mid-Atlantic Ridge (36°–39°N) and the Azores hotspot. Journal of Geophysical Research 106 (B10), 21719–21735.

Flewellen, C., Millard, N., Rouse, I., 1994. Swath bathymetry on the TOBI vehicle. BRIDGE Newsletter 6, 26–28.

Fornari, D.J., Ryan, W.B.F., 1984. The evolution of craters and calderas on young seamounts: insights from Sea MARC I and Sea Beam sonar surveys of a small group near the axis of the East Pacific Rise at ~10N. Journal of Geophysical Research 89, 11069–11083.

German, C.R., Parson, L.M., HEAT Scientific Team, 1996. Hydrothermal exploration near the Azores Triple Junction: tectonic control of venting at slow spreading ridges? Earth and Planetary Science Letters 138 (1–4), 93–104.

Gracia, E., Charlou, J.L., Radford-Knoery, J., Parson, L.M., 2000. Non-transform offsets along the Mid-Atlantic Ridge south of the Azores (38°N–34°N): ultramafic exposures and hosting of hydrothermal vents. Earth and Planetary Science Letters 177 (1–2), 89–103.

Gregg, T.K.P., Fink, J.H., 1995. Quantification of submarine lava-flow morphology through analog experiments. Geology 23, 73–76.

Gregg, T.P.K., Fornari, D.J., 1998. Long submarine lava flows: observations and results from numerical modelling. Journal of Geophysical Research 103 (B11), 27517–27531.

Griffiths, R.W., Fink, J.H., 1992. Solidification and morphology of submarine lavas: a dependence on extrusion rate. Journal of Geophysical Research 97, 19729–19737.

Griffiths, R.W., Fink, J.H., 1993. Effects of surface cooling on the spreading of lava flows and domes. Journal of Fluid Mechanics 252, 667–702.

Grosfils, E., Aubele, J., Crumpler, L., Gregg, T., Sakimoto, S., 2000. Volcanism on Venus and Earth's seafloor. In: Gregg, T., Zimbelman, J. (Eds.), Environmental Effects on Volcanic Eruptions: From the Deep Ocean to Deep Space. Plenum Publishers, New York, pp. 113–142.

Head, J.W., Wilson, L., 2003. Deep submarine pyroclastic eruptions: theory and predicted landforms and deposits. Journal of Volcanological and Geothermal Research 121, 155–193.

Head, J.W., Wilson, L., Smith, D.K., 1996. Mid-ocean ridge eruptive vent morphology and substructure: evidence for the dike widths, eruption rates, and axial volcanic ridges. Journal of Geophysical Research 101, 28265–28280.

Hekinian, R., Pineau, F., Shilobreeva, S., Bideau, D., Gracia, E., Javoy, M., 2000. Deep sea explosive activity on the Mid-Atlantic Ridge near 34°50′N: magma composition, vesicularity, and volatile content. Journal of Volcanological and Geothermal Research 98, 49–77.

Jordan, T.H., Menard, H.W., Smith, D.K., 1983. Density and size distribution of seamounts in the eastern Pacific inferred from wide beam sounding data. Journal of Geophysical Research 88, 10508–10518.

Kennish, M.J., Lutz, R.A., 1998. Morphology and distribution of lava flows on mid-ocean ridges: a review. Earth-Science Reviews 43, 63–90.

Kong, L.S.L., Detrick, R.S., Fox, P.J., Mayer, L.A., Ryan, W.B.F., 1988. The morphology and tectonics of the Mark area from Sea Beam and Sea MARC I observations (Mid Atlantic Ridge 23°). Marine Geophysical Researches 10, 59–90.

Langmuir, C.H., Klein, E.M., Plank, T., 1992. Petrological systematics of mid-ocean ridge basalts: constraints on melt generation beneath ocean ridges. In: Morhan, J.P., Blackman, D.K., Sinton, J.M. (Eds.), Mantle Flow and Melt Generation at Mid Ocean Ridges. Geophysical Monograph, vol. 71. American Geophysical Union, pp. 183–280.

Leslie, S.C., Moore, G.F., Morgan, J.K., 2004. Internal structure of Puna Ridge: evolution of the submarine East Rift Zone of Kilauea Volcano, Hawai'i. Journal of Volcanology and Geothermal Research 129 (4), 237–259.

Ligi, M., Mitchell, N.C., Marani, M., Gamberi, F., Pentitenti, D., Carrara, G., Rovere, M., Portaro, R., Centorami, G., Bortoluzzi, G., Jacobs, C., Rouse, I., Flewellen, C., Whittle, S., Terrinha, P., Freire-Luis, J., Lourenco, N., 1999. Giant volcanic ridges amongst the Azores Islands. Presented at Fall meeting of the American Geophysical Union.

Litvin, V.M., 1984. The Morphostructure of the Atlantic Ocean Floor. D. Reidel Publishing Company, Dordrecht.

Lourenco, N., Miranda, J.M., Luis, J.F., Victor, L.A.M., Madeira, J., Needham, H.D., 1998. Morpho-tectonic analysis of the Azores Volcanic Plateau from a new bathymetric compilation of the area. Marine Geophysical Researches 20, 141–156.

Luis, J.F., Miranda, J.M., Galdeano, A., Patriat, P., 1998. Constraints on the structure of the Azores spreading centre from gravity data. Marine Geophysical Researches 20 (3), 157–170.

MacDonald, K.C., Haymon, R.M., Miller, S.P., Sempere, J.C., Fox, P. J., 1988. Deep tow and Sea Beam studies of duelling propagating ridges on the East Pacfic Rise near 2040′S. Journal of Geophysical Research 93, 2875–2898.

Magde, L.S., Smith, D.K., 1995. Seamount volcanism at the Reykjanes Ridge: relationship to the Iceland hot spot. Journal of Geophysical Research 100, 8449–8468.

Masson, D.G., Millard, N.W., 1991. TOBI: a new development in deep-ocean geological mapping. NERC–News 17, 11–13 (April).

Mendel, V., Sauter, D., 1997. Seamount volcanism at the super slow spreading Southwest Indian Ridge between 57°E and 70°E. Geology 25 (2), 99–102.

Miranda, J.M., Luis, J.F., Abreu, I., Victor, L.A.M., 1991. Tectonic framework of the Azores. Geophysical Research Letters 18, 1421–1424.

Miranda, J.M., Victor, L.A.M., Simoes, J.Z., Luis, J.F., Matias, L., Shimamura, H., Shiobara, H., Nemoto, H., Mochizuki, H., Hirn, A., Lepine, J.C., 1998. Tectonic setting of the Azores Plateau deduced from an OBS survey. Marine Geophysical Researches 20, 171–182.

Mitchell, N.C., 2003. Susceptibility of mid-ocean ridge volcanic islands and seamounts to large scale landsliding. Journal of Geophysical Research 108, doi:10.1029/2002JB001997.

Mitchell, N.C., Livermore, R.A., 1998. Speiss Ridge: an axial high on the slow-spreading Southwest Indian Ridge. Journal of Geophysical Research 103, 15457–15471.

Mitchell, N.C., Schmitt, T., Isidro, I., Tempera, F., Cardigos, F., Nunes, J.C., Figueiredo, 2003a. Multibeam sonar survey of the central Azores volcanic islands. InterRidge News 12 (2), 30–32.

Mitchell, N.C, Dade, W.B., Masson, D.G., 2003b. Erosion of the submarine flanks of the Canary Islands. Journal of Geophysical Research 108, doi:10.1029/2002JF000003.

Moreira, M., Allegre, C., 2002. Rare gas systematics on Mid-Atlantic Ridge (37–40N). Earth and Planetary Science Letters 198, 401–416.

Murton, B.J., Rouse, I.P, Millard, N.W., 1992. Multisensor deep towed instrument explores ocean floor. EOS, Transactions of the American Geophysical Union 73 (20) 225, 288.

Nunes, J.C.C., 2002. Unpublished PhD thesis. A actividade vulcanica na Ilha do Pico do Plistocenico superior ao Holocenico: mecanismo eruptivo e hazard vulcanico. University of Azores.

Ondreas, H., Fouquet, Y., Voisset, M., Radford-Knoery, J., 1997. Detailed study of three continuous segments of the Mid-Atlantic Ridge, South of the Azores (37°N to 38°30′N) using acoustic imaging coupled with submersible observations. Marine Geophysical Researches 19, 231–255.

Parson, L.M., Murton, B.J., Searle, R.C., Booth, D., Evans, J., Field, P., Keeton, J., Laughton, A., McAlister, E., Millard, N., Redbourne, L., Rouse, I., Shor, A., Smith, D., Spencer, S., Summerhayes, C., Walker, C., 1993. En echelon axial volcanic ridges at the Reykjanes Ridge: a life cycle of volcanism and tectonics. Earth and Planetary Science Letters 117, 73–87.

Parson, L., Murton, B., Searle, R., Pierce, C., Allerton, S., Sinha, M., Spencer, S., Cann, J., Livermore, R., 1999. Slices of Ridge. BRIDGE Newsletter 17, 12–13.

Parson, L.M., Gracia, E., Coller, D., German, C., Needham, D., 2000. Second-order segmentation; the relationship between volcanism and tectonism at the MAR, 38°N–35°40′N. Earth and Planetary Science Letters 178 (3–4), 231–251.

Perfit, M.R., Davidson, J.P., 2000. Plate tectonics and volcanism. In: Sigurdsson, H., Houghton, B., McNutt, S.R., Rymer, H., Stix, J. (Eds.), Encyclopedia of Volcanoes. Academic Press, San Diego, CA, pp. 89–113.

Rabain, A., Cannat, M., Escartin, J., Pouliquen, G., Deplus, C., Rommevaux-Jestin, C., 2001. Focused volcanism and growth of a slow spreading segment (Mid-Atlantic Ridge, 35°N). Earth and Planetary Science Letters 185 (1–2), 211–224.

Ruiz, C.R., Garcia-Cacho, L., Arana, V., Luque, A.Y., Felpeto, A., 2000. Submarine volcanism surrounding Tenerife, Canary Islands: implications for tectonic controls, and oceanic shield forming processes. Journal of Volcanology and Geothermal Research 103 (1–4), 105–119.

Sauter, D., Parson, L., Mendel, V., Rommevaux-Jestin, C., Gomez, O., Briais, A., Mevel, C., Tamaki, K., the FUJI scientific team, 2002. TOBI sidescan sonar imagery of the very slow spreading southwest Indian ridge: evidence for along-axis magma distribution. Earth and Planetary Science Letters 199, 81–95.

Scheirer, D.S., Macdonald, K.C., 1995. Near-axis seamounts on the flanks of the East Pacific Rise, 8°N to 17°N. Journal of Geophysical Research 100, 2239–2259.

Searle, R.C., 1980. Tectonic pattern of the Azores spreading center and triple junction. Earth and Planetary Science Letters 51, 415–434.

Searle, R.C., Mitchell, N.C., Escartin, J., Slootweg, A.P., Russell, S. M., Cowie, P.A., Allerton, S., MacLeoad, C.J., 1997. Tectonic strain and recent evolution of the broken spur segment Mid-Atlantic Ridge 29°N. BRIDGE Newsletter 13, 58.

Searle, R.C., Cowie, P.A., Mitchell, N.C., Allerton, S., MacLeoad, C. J., Escartin, J., Russell, S.M., Slootweg, A.P., Tanaka, T., 1998. Fault structure and detailed evolution of a slow-spreading ridge segment: the Mid-Atlantic Ridge at 29°N. Earth and Planetary Science Letters 154, 167–183.

Sempere, J.C., Macdonald, K.C., 1986. Deep tow studies of the overlapping spreading centres at 9°3′N on the East Pacific Rise. Tectonics 5, 881–900.

Smith, D.K., 1996. Comparison of the shapes and sizes of seafloor volcanoes on Earth and pancake domes on Venus. Journal of Volcanological and Geothermal Research 73, 47–64.

Smith, D.K., 1988. Shape analysis of Pacific seamounts. Earth and Planetary Science Letters 90, 457–466.

Smith, D.K., Cann, J.R., 1990. Hundreds of small volcanoes on the median valley of the Mid-Atlantic Ridge at 24–30°N. Nature 348, 152–155.

Smith, D.K., Cann, J.R., 1992. The role of seamount volcanism in crustal construction at the Mid-Atlantic Ridge (24°–30°N). Journal of Geophysical Research 97, 1645–1658.

Smith, D.K., Cann, J.R., 1999. Constructing the upper crust of the Mid-Atlantic Ridge: a reinterpretation based on the Puna Ridge, Kilauea Volcano. Journal of Geophysical Research 104 (B11), 25379–25399.

Smith, D.K., Jordan, T.H., 1988. Seamount statistics in the Pacific Ocean. Journal of Geophysical Research 93, 2899–2918.

Smith, D.K., Cann, J.R., Dougherty, M.E., Lin, J., Spencer, S., Macleod, C., Keeton, J., McAllister, E., Brooks, B., Pascoe, R., Robertson, W., 1995a. Mid-Atlantic Ridge volcanism from deep-towed side scan sonar images 25°–29°N. Journal of Volcanology and Geothermal Research 67, 233–262.

Smith, D.K., Humphris, S.E., Bryan, W.B., 1995b. A comparison of volcanic edifices at the Reykanes Ridge and the Mid-Atlantic Ridge at 24°–30°N. Journal of Geophysical Research 100, 22485–22498.

Smith, D.K., Humphris, S.E., Tivey, M.A., Cann, J.R., 1997. Viewing the morphology of the Mid-Atlantic Ridge from a new perspective. EOS, Transactions of the American Geophysical Union 78: 265, 269.

Smith, D.K., Tivey, M.A., Gregg, P.M., Kong, L.S.L., 2001. Magnetic anomalies at the Puna Ridge, a submarine extension of Kilauea Volcano: implications for lava deposition. Journal of Geophysical Research 106 (B8), 16047–16060.

Smith, D.K., Kong, L.S.L., Johnson, K.T.M., Reynolds, J.R., 2002. Volcanic morphology of the submarine Puna Ridge, Kilauea Volcano. In: Takahashi, E., Lipman, P.W., Garcia, M.J., Naka, J., Aramaki, S. (Eds.), Hawai‘ian Volcanoes, Deep Underwater Perspectives. Geophysical Monograph, vol. 128. American Geophysical Union, Washington.

Thibaud, R., Gente, P., Maia, M., 1998. A systematic analysis of the Mid-Atlantic Ridge: morphology and gravity between 15°N and 40°N: constraints on thermal structure. Journal of Geophysical Research 103 (B10), 24223–24243.

Wadge, G., Cross, A., 1988. Quantitative methods for detecting aligned points: an application to the volcanic vents of the Michoacan–Guanajuanto volcanic field, Mexico. Geology 16, 815–818.

Walker, G.P.L., 1991. Structure, and origin y injection of lava under surface crust, of tumuli, “lava rises”, “lava-rise pits”, and “lava-inflation clefts” in Hawai‘i. Bulletin of Volcanology 53, 546–558.

Whitesides, G., 2000. Volcanic edifices of the Pico submarine ridge in the Azores: a morphological analysis based on TOBI sidescan sonar and bathymetry. MPhil dissertation, Department of Geography, University of Cambridge.

Woodhall, 1974. Geology and history of Pico Island, Azores. Nature 248, 663–665.

Zhang, Y.S., Tanimoto, R., 1992. Ridges, hotspots and their interaction as observed in seismic maps. Nature 355, 45–49.

Zhu, W., Smith, D.K., Montesi, L.G.J., 2002. Effects of regional slope on viscous flows: a preliminary study of lava terrace emplacement at submarine volcanic rift zones. Journal of Volcanology and Geothermal Research 119, 145–159.